

Fine Particulate Matter Induces Childhood Asthma Attacks via Extracellular Vesicle-Packaged Let-7i-5p-Mediated Modulation of the MAPK Signaling Pathway

Rui Zheng, Mulong Du, Man Tian, Zhaozhong Zhu, Chengcheng Wei, Haiyan Chu, Cong Gan, Jiayuan Liang, Renjie Xue, Fang Gao, Zhenguang Mao, Meilin Wang,* and Zhengdong Zhang*

Fine particulate matter less than 2.5 μm in diameter ($\text{PM}_{2.5}$) is a major risk factor for acute asthma attacks in children. However, the biological mechanism underlying this association remains unclear. In the present study, $\text{PM}_{2.5}$ -treated HBE cells-secreted extracellular vesicles ($\text{PM}_{2.5}$ -EVs) caused cytotoxicity in “horizontal” HBE cells and increased the contractility of “longitudinal” sensitive human bronchial smooth muscle cells (HBSMCs). RNA sequencing showed that let-7i-5p is significantly overexpressed in $\text{PM}_{2.5}$ -EVs and asthmatic plasma; additionally, its level is correlated with $\text{PM}_{2.5}$ exposure in children with asthma. The combination of EV-packaged let-7i-5p and the traditional clinical biomarker IgE exhibits the best diagnostic performance (area under the curve [AUC] = 0.855, 95% CI = 0.786–0.923). Mechanistically, let-7i-5p is packaged into $\text{PM}_{2.5}$ -EVs by interacting with ELAVL1 and internalized by both “horizontal” recipient HBE cells and “longitudinal” recipient-sensitive HBSMCs, with subsequent activation of the MAPK signaling pathway via suppression of its target *DUSP1*. Furthermore, an injection of EV-packaged let-7i-5p into $\text{PM}_{2.5}$ -treated juvenile mice aggravated asthma symptoms. This comprehensive study deciphered the remodeling of the extracellular environment mediated by the secretion of let-7i-5p-enriched EVs during $\text{PM}_{2.5}$ -induced asthma attacks and identified plasma EV-packaged let-7i-5p as a novel predictor of childhood asthma.

1. Introduction

Asthma is a common chronic respiratory disease characterized by airway hyperresponsiveness, airway inflammation and reversible airway remodeling.^[1,2] Globally, asthma remains a serious health problem that affects 358 million individuals, especially among children.^[3,4] Clinically, asthma attacks in children lead to reversible and repeated attacks of coughing, wheezing, shortness of breath, and chest tightness, thereby impairing quality of life and imposing a heavy burden on the family and community.^[5]


As environmental pollution is predictable and preventable, airborne fine particulate matter <2.5 μm in diameter ($\text{PM}_{2.5}$) has been considered a crucial type of allergen causing acute asthma attacks in children.^[5–7] Here, two airway cell types ultimately responsible for asthma pathogenesis are considered: human bronchial epithelial (HBE) cells, which form the first barrier between the external environment and the internal bronchus and are the major

R. Zheng, C. Wei, H. Chu, J. Liang, F. Gao, Z. Mao, M. Wang, Z. Zhang
Department of Genetic Toxicology
The Key Laboratory of Modern Toxicology of Ministry of Education
Center for Global Health
School of Public Health
Nanjing Medical University
Nanjing 211166, China
E-mail: mawang@njmu.edu.cn; drzdzhang@njmu.edu.cn

R. Zheng, M. Du, C. Wei, H. Chu, J. Liang, Z. Mao, M. Wang, Z. Zhang
Department of Environmental Genomics
Jiangsu Key Laboratory of Cancer Biomarkers, Prevention and Treatment
Collaborative Innovation Center for Cancer Personalized Medicine
Nanjing Medical University
Nanjing 211166, China

M. Du
Department of Biostatistics
Center for Global Health
School of Public Health
Nanjing Medical University
Nanjing 211166, China

M. Tian, C. Gan, R. Xue
Department of Respiratory Medicine
Children's Hospital of Nanjing Medical University
Nanjing 210008, China

 The ORCID identification number(s) for the author(s) of this article can be found under <https://doi.org/10.1002/advs.202102460>

© 2021 The Authors. Advanced Science published by Wiley-VCH GmbH. This is an open access article under the terms of the Creative Commons Attribution License, which permits use, distribution and reproduction in any medium, provided the original work is properly cited.

DOI: 10.1002/advs.202102460

target of inhaled particles and pathogens,^[8] and human bronchial smooth muscle cells (HBSMCs) located below HBE cells, which are the main effectors of bronchial contraction and whose excessive contraction induces airway hyperresponsiveness.^[9] Emerging evidence has shown that various stimuli (i.e., air pollutants, allergens and viruses) stimulate HBE cells to recruit effector T cells and trigger T helper 2 (Th2) cytokine secretion, which affects both HBE cells and HBSMCs via a feedback loop and further increases cytotoxicity in HBE cells and HBSMC contractility.^[10] However, the complex mechanism of asthma pathogenesis, especially the intercellular communication between HBE cells and HBSMCs, is incompletely elucidated. Hence, an exploration of comprehensive mechanisms contributing to PM_{2.5}-induced childhood asthma is urgently needed.

Recently, extracellular vesicles (EVs) have been regarded as important messengers in intercellular communication. EVs have been reported to be released by multiple types of cells under physiological or pathological conditions^[11,12] and then transfer intracellular cargos (i.e., nucleic acids, lipids and proteins) from the parent cells to recipient cells, thereby modulating the biological functions of the recipient cells.^[13,14] Regarding the above-mentioned EV-packaged cargos, emerging studies have noted that microRNAs (miRNAs) are considered novel tools to investigate the pathologic mechanisms and biomarkers of asthma.^[15] Moreover, PM_{2.5} exposure regulates miRNA expression profiles in airway cells.^[16,17] Based on these data, EV-packaged miRNAs may function as important extracellular messengers in the PM_{2.5}-stimulated airway microenvironment. However, the role of EV-packaged miRNAs in PM_{2.5}-induced childhood asthma remains unknown.

In the present study, we found that PM_{2.5}-treated HBE cells released EVs containing aberrantly expressed let-7i-5p that were taken up by normal HBE cells in the “horizontal” orientation and sensitive HBSMCs in the “longitudinal” orientation, leading to cytotoxicity and airway hyperresponsiveness, respectively. Accumulating studies have reported a role for let-7i-5p in multiple diseases.^[18–20] For example, the low expression of let-7i-5p caused by histone deacetylase 6 (HDAC6) directly increased expression levels of the target gene *TSP1* levels, thereby suppressing antiphagocytic and neoplastic behaviors of hepatocellular carcinoma.^[21] However, the biological function of let-7i-5p in PM_{2.5}-induced childhood asthma is unclear. Our study highlights the intercellular communication mechanism of EV-packaged let-

7i-5p-mediated asthma and identifies EV-packaged let-7i-5p as a novel predictor of PM_{2.5}-induced asthma.

2. Results

2.1. EVs Secreted by PM_{2.5} Stimulation “Horizontally” Induce Cytotoxicity in HBE Cells

The flowchart of the evaluation strategy for EVs is presented in **Figure 1A**. First, we performed a direct PM_{2.5} exposure assay and found that PM_{2.5} dose-dependently decreased the viability of HBE cells after exposure for different times (Table S1, Supporting Information). Compared with the PM_{2.5} group exposed for 12 h, PM_{2.5} concentrations greater than or equal to 250 μg mL⁻¹ exhibited a significant difference in their ability to reduce the number of HBE cells after treatment for 24 or 48 h (Figure 1B). Because the concentration of PM_{2.5} may be up to 100–200 μg m⁻³ in winter, combined with children’s daily inhalation of 10 m³ of air and the average volume of 6.2 mL of fluid in the lungs and airway, the corresponding PM_{2.5} concentration was calculated to be 161–323 μg mL⁻¹.^[22] We selected 250 μg mL⁻¹ PM_{2.5} and an exposure time of 24 h as the PM_{2.5} treatment conditions in this study to account for children exposed to high levels of PM_{2.5}. As shown in Figure 1C,D, PM_{2.5} significantly induced apoptosis and G1/G2 arrest in normal HBE cells. Thus, PM_{2.5} exposure is cytotoxic to normal HBE cells.

Next, after coculture of normal and PM_{2.5}/NC-treated HBE cells in a Transwell plate for 24 h, the culture medium of PM_{2.5}-treated HBE cells exerted stronger cytotoxic effects than those observed on normal HBE cells exposed to NC-treated HBE cells (Figure S1, Supporting Information), suggesting that PM_{2.5}-treated HBE cells may secrete EVs to induce cytotoxicity in HBE cells. Using visualization approaches, we found that EVs purified from the culture medium of PM_{2.5}/NC-treated HBE cells (PM_{2.5}/NC-EVs) exhibited a typical cup-shaped morphology, were ≈100 nm in size, expressed the typical EV markers CD63, TSG101 and Alix, and lacked cellular contaminants such as calnexin and Grp94 (Figure 1E–G and Figure S2, Supporting Information). Fluorescence microscopy showed PKH67 green fluorescent dye in the cytoplasm of HBE cells, while no PKH67 green fluorescent dye was observed in the non-EVs group, indicating that PM_{2.5}/NC-EVs were taken up by normal HBE cells (Figure 1H). However, this ability was abolished by inhibiting endocytosis with cytochalasin D (Figure S3, Supporting Information), indicating the efficient transportability of the secreted EVs. Subsequently, direct incubation with PM_{2.5}-EVs for 24 h markedly decreased HBE cell viability, promoted apoptosis, and stimulated S phase arrest (Figure 1I–L). Moreover, these aberrant cellular activities were rescued by the pharmacological inhibition of EV secretion with GW4869 (Figure 1I and Figure S4, Supporting Information). Taken together, these findings indicate that EVs secreted by PM_{2.5}-stimulated HBE cells are “horizontally” transported into normal HBE cells, with subsequent induction of cytotoxicity.

2.2. EVs Secreted Following PM_{2.5} Stimulation “Longitudinally” Promote the Contractility of Sensitive HBSMCs

As PM_{2.5}-EVs may be “longitudinally” transported into normal HBSMCs, we detected the contractility of these cells by evaluating

Z. Zhu
Department of Emergency Medicine
Massachusetts General Hospital and Harvard Medical School
Boston, MA 02114, USA

F. Gao
Key Laboratory of Environmental Medicine Engineering
Ministry of Education of China
School of Public Health
Southeast University
Nanjing 210009, China

M. Wang
The Affiliated Suzhou Hospital of Nanjing Medical University
Suzhou Municipal Hospital, Gusu School
Nanjing Medical University
Suzhou 215008, China

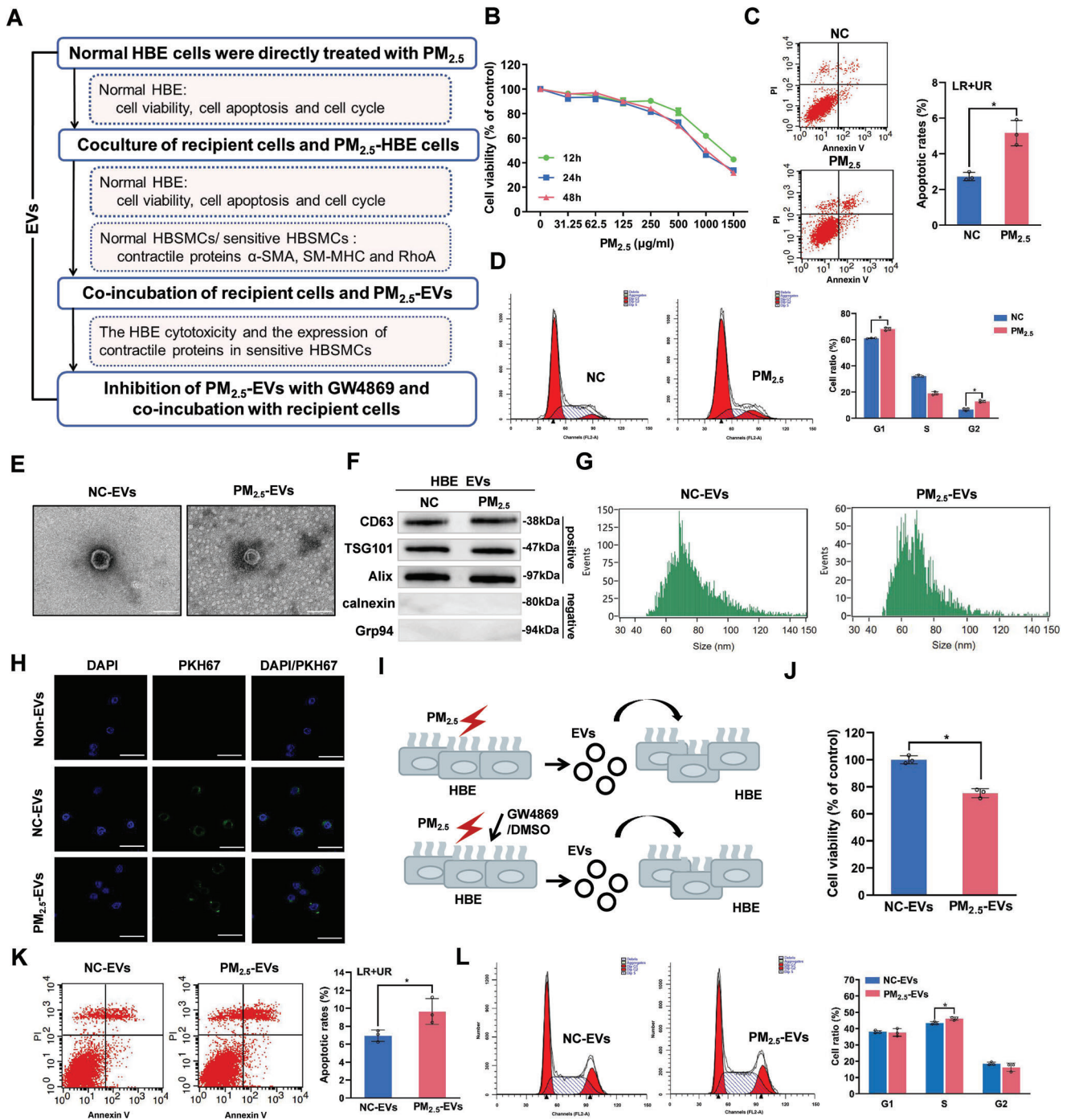


Figure 1. The effect of PM_{2.5}-EVs on cytotoxicity in HBE cells. PM_{2.5}-treated HBE cells were designated PM_{2.5}-HBE cells. EVs isolated from PM_{2.5}-treated HBE cells and NC-treated HBE cells were designated PM_{2.5}-EVs and NC-EVs, respectively. A) Flowchart of the strategy used to evaluate the effect of PM_{2.5}-EVs on cytotoxicity in HBE cells and the contractility of sensitive HBSMCs. B) The viability of HBE cells was evaluated using a CCK-8 assay after PM_{2.5} treatment. C) The apoptosis of HBE cells was assessed using flow cytometry after PM_{2.5} treatment. D) The cell cycle of HBE cells was analyzed using flow cytometry after PM_{2.5} treatment. E) Purified PM_{2.5}/NC-EVs were identified using TEM. Scale bar, 100 nm. F) The EV-specific markers (CD63, TSG101 and Alix) and negative controls (calnexin and Grp94) were evaluated using Western blotting. G) The size distributions of PM_{2.5}/NC-EVs were confirmed using NanoFCM. H) Representative fluorescence images of HBE cells after an incubation with PM_{2.5}/NC-EVs labelled with PKH67 (green) or non-EVs. Scale bar, 25 µm. I) Schematic illustration of HBE cells incubated with PM_{2.5}-EVs or PM_{2.5}-EVs pretreated with DMSO/GW4869. J) The viability of HBE cells was evaluated using a CCK-8 assay after an incubation with PM_{2.5}/NC-EVs. K) The apoptosis of HBE cells was assessed using flow cytometry after an incubation with PM_{2.5}/NC-EVs. L) The cell cycle of HBE cells was analyzed using flow cytometry after an incubation with PM_{2.5}/NC-EVs. Statistical significance was assessed using two-tailed Student's *t*-test. Values represent means ± SD. **p* < 0.05.

the expression of three identified vital proteins that regulate HBSMC contractility: α -smooth muscle actin (α -SMA), smooth muscle myosin heavy chain 11 (SM-MHC) and RhoA (Figure 1A). No differences in the expression of contractile proteins were observed in normal HBSMCs after coculture with PM_{2.5}-treated HBE cells (Figure 2A and Figure S5A, Supporting Information). Although PKH67-labelled PM_{2.5}/NC-EVs were transferred into normal HBSMCs (Figure 2B and Figure S6, Supporting Information), PM_{2.5}-EVs did not regulate the expression of contractile proteins (Figure 2C,D). Based on these data, PM_{2.5} exposure may function as an inducing factor rather than an initiating factor of asthma by causing airway hyperresponsiveness and subsequently inducing asthma attacks. To simulate the condition of HBSMCs during asthma remission, we established a sensitive HBSMC model by using 100 ng mL⁻¹ IL-13 and found that sensitive HBSMCs exhibited increased eotaxin expression (Figure 2E). Compared with NC-treated HBE cells, sensitive HBSMCs cocultured with PM_{2.5}-treated HBE cells showed higher expression levels of contractile proteins (Figure 2F and Figure S5B, Supporting Information). Similarly, “longitudinal” recipient-sensitive HBSMCs displayed efficient uptake of PKH67-labelled PM_{2.5}/NC-EVs (Figure 2G, and Figure S7, Supporting Information) and exhibited increased expression of contractile proteins after treatment with PM_{2.5}-EVs (Figure 2H and Figure S5C, Supporting Information). In contrast, GW4869 treatment of PM_{2.5}-treated HBE cells reduced the expression levels of contractile proteins in “longitudinal” recipient-sensitive HBSMCs (Figure 2I and Figure S5D, Supporting Information). Collectively, these results suggest that PM_{2.5}-EVs are also “longitudinally” delivered to sensitive HBSMCs, enhancing their contractility.

2.3. EV-Packaged Let-7i-5p Correlates with PM_{2.5} Exposure in Children with Asthma

Aiming to explore the epigenetic regulation of PM_{2.5}-induced childhood asthma, we verified EVs isolated from plasma in children (Figure 3A and Figure S8, Supporting Information) and performed RNA sequencing on EV-packaged miRNAs in plasma samples from children and PM_{2.5}/NC-treated HBE cells (Figure 3B). As shown in Figure 3C, 262 EV-packaged miRNAs were differentially expressed in PM_{2.5}-EVs compared with NC-EVs (118 upregulated and 144 downregulated; |fold change| > 2, $P_{\text{adj}} < 0.05$), and 173 EV-packaged miRNAs (113 upregulated and 60 downregulated; |fold change| > 2, $P_{\text{adj}} < 0.05$) were differentially expressed in the comparison of plasma from children with asthma and healthy controls. Furthermore, we identified 11 overlapping upregulated EV-packaged miRNAs in the cell models and plasma from children (Figure 3D), among which the most abundant EV-packaged miRNA, let-7i-5p, was selected as the candidate miRNA for further verification (Figure 3E). Consistent with the RNA sequencing results, the level of EV-packaged let-7i-5p was approximately two-fold higher in PM_{2.5}-EVs than in NC-EVs (Figure S9, Supporting Information). We confirmed the existing pattern of extracellular let-7i-5p by treating cells with RNaseA/Triton X-100 and found that the level of let-7i-5p in the culture medium of PM_{2.5}-treated HBE cells did not change after RNaseA treatment but decreased markedly when RNaseA and Triton X-100 were added simultaneously (Figure 3F). However, the let-

7i-5p level was reduced in the culture medium of NC-treated HBE cells after treatment with RNaseA. Additional EV inhibition experiments verified that the level of let-7i-5p in the culture medium of PM_{2.5}-treated HBE cells was significantly reduced after treatment with GW4869 (Figure 3G). Based on these results, extracellular let-7i-5p is mainly encapsulated in EVs instead of directly secreted.

Next, we sought to examine the association of EV-packaged let-7i-5p with childhood asthma attacks and PM_{2.5} exposure based on 55 patients and 55 healthy controls (Figure 3H). The EV-packaged let-7i-5p level remained stable after different freeze-thaw cycles (Figure S10A, Supporting Information) and room temperature incubation periods (Figure S10B, Supporting Information). Compared with the healthy controls (Table S2, Supporting Information), children with asthma had significantly higher plasma total IgE levels and peripheral blood eosinophil percentages ($p < 0.001$) and were exposed to higher levels of PM_{2.5}. We further detected let-7i-5p levels in plasma EVs from children and found that the expression of EV-packaged let-7i-5p was significantly increased in children with asthma (Figure 3I). Moreover, EV-packaged let-7i-5p exhibited a high capacity to discriminate children with asthma from healthy controls, with an area under the curve (AUC) of 0.785 (95% confidence interval [CI] = 0.701–0.869; Figure 3J). Notably, the AUC of the combination of IgE and EV-packaged let-7i-5p was increased to 0.855 (95% CI = 0.786–0.923), accompanied by increases in the sensitivity and specificity to 70.90% and 85.20%, respectively (Figure 3J). Correlation analysis revealed that the EV-packaged let-7i-5p level exhibited a significant positive correlation with PM_{2.5} exposure in children with asthma but not in healthy controls (Figure 3K and Figure S11, Supporting Information). These observations imply that plasma levels of EV-packaged let-7i-5p may be a biomarker for PM_{2.5}-induced asthma in children.

2.4. EV-Packaged Let-7i-5p Affects Cytotoxicity in HBE Cells and the Contractility of Sensitive HBSMCs

We first transfected the let-7i-5p mimic into recipient cells to further determine the biological significance of EV-packaged let-7i-5p in cytotoxicity in HBE cells and the contractility of sensitive HBSMCs and found that let-7i-5p overexpression reduced HBE cell growth, induced an increase in the apoptosis rate of HBE cells, and promoted S phase arrest (Figure S12A–D, Supporting Information). Moreover, let-7i-5p overexpression markedly increased the expression of contractile proteins in sensitive HBSMCs (Figure S12E,F, Supporting Information). Next, we cocultured HBE cells transfected with Cy3-labelled let-7i-5p mimic with recipient cells and observed the red fluorescence of the labelled let-7i-5p in both “horizontal” recipient HBE cells and “longitudinal” recipient-sensitive HBSMCs, indicating that EV-packaged let-7i-5p was taken up by recipient cells (Figure S13A, Supporting Information). Subsequently, we evaluated the level of let-7i-5p after incubating the recipient cells with EVs and found that the cellular let-7i-5p levels were increased upon incubation with PM_{2.5}-EVs but not upon incubation with NC-EVs or direct exposure to PM_{2.5} (Figure S13B,C, Supporting Information). These findings indicate that the enriched let-7i-5p in recipient cells is mainly transported by PM_{2.5}-EVs. We further examined the

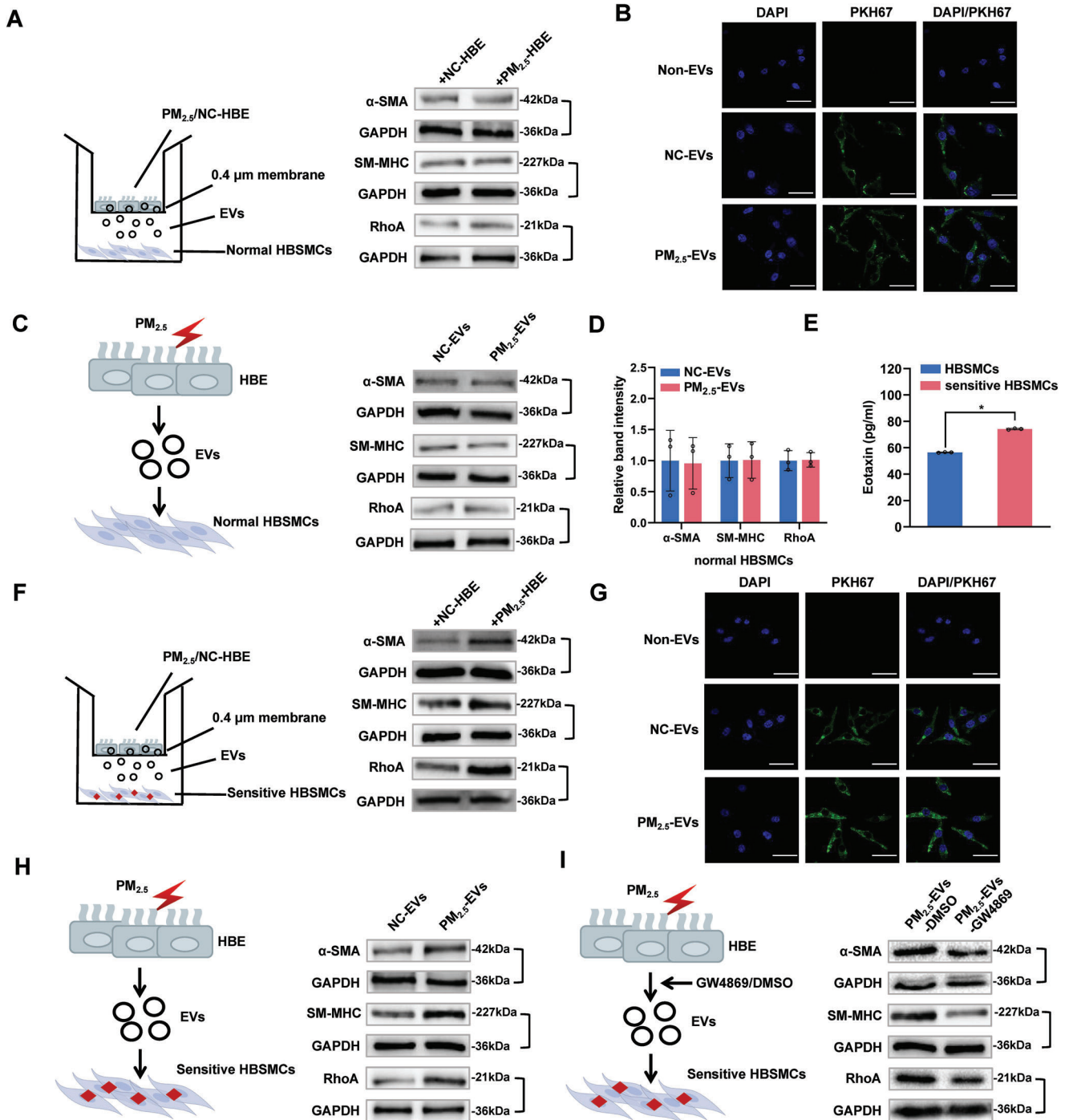


Figure 2. Effect of PM_{2.5}-EVs on the contractility of sensitive HBSMCs. The PM_{2.5}/NC-treated HBE cells are designated PM_{2.5}/NC-HBE cells. The red lightning signal represents PM_{2.5} exposure. A) The levels of the contractile proteins α-SMA, SM-MHC and RhoA in normal HBSMCs cocultured with PM_{2.5}/NC-HBE cells were analyzed using Western blotting. B) Representative fluorescence images of normal HBSMCs after an incubation with PM_{2.5}/NC-EVs labelled with PKH67 (green) or non-EVs. Scale bar, 25 μm. C) The levels of the contractile proteins α-SMA, SM-MHC and RhoA in normal HBSMCs incubated with PM_{2.5}/NC-EVs were analyzed using Western blotting. D) The band intensity of contractile proteins in normal HBSMCs incubated with PM_{2.5}/NC-EVs. E) Normal HBSMCs were treated with IL-13 to establish a sensitive HBSMC model. The expression of eotaxin in normal and sensitive HBSMCs was measured using an enzyme-linked immunosorbent assay (ELISA) kit. F) The levels of the contractile proteins α-SMA, SM-MHC and RhoA in sensitive HBSMCs cocultured with PM_{2.5}/NC-HBE cells were analyzed using Western blotting. G) Representative fluorescence images of sensitive HBSMCs after an incubation with PM_{2.5}/NC-EVs labelled with PKH67 (green) or non-EVs. Scale bar, 25 μm. H) The contractile proteins α-SMA, SM-MHC and RhoA in sensitive HBSMCs incubated with PM_{2.5}/NC-EVs were analyzed using Western blotting. I) The contractile proteins α-SMA, SM-MHC and RhoA in sensitive HBSMCs incubated with PM_{2.5}/NC-EVs pretreated with DMSO/GW4869 were analyzed using Western blotting. Statistical significance was assessed using two-tailed Student's *t*-test. Values represent means ± SD. **p* < 0.05.

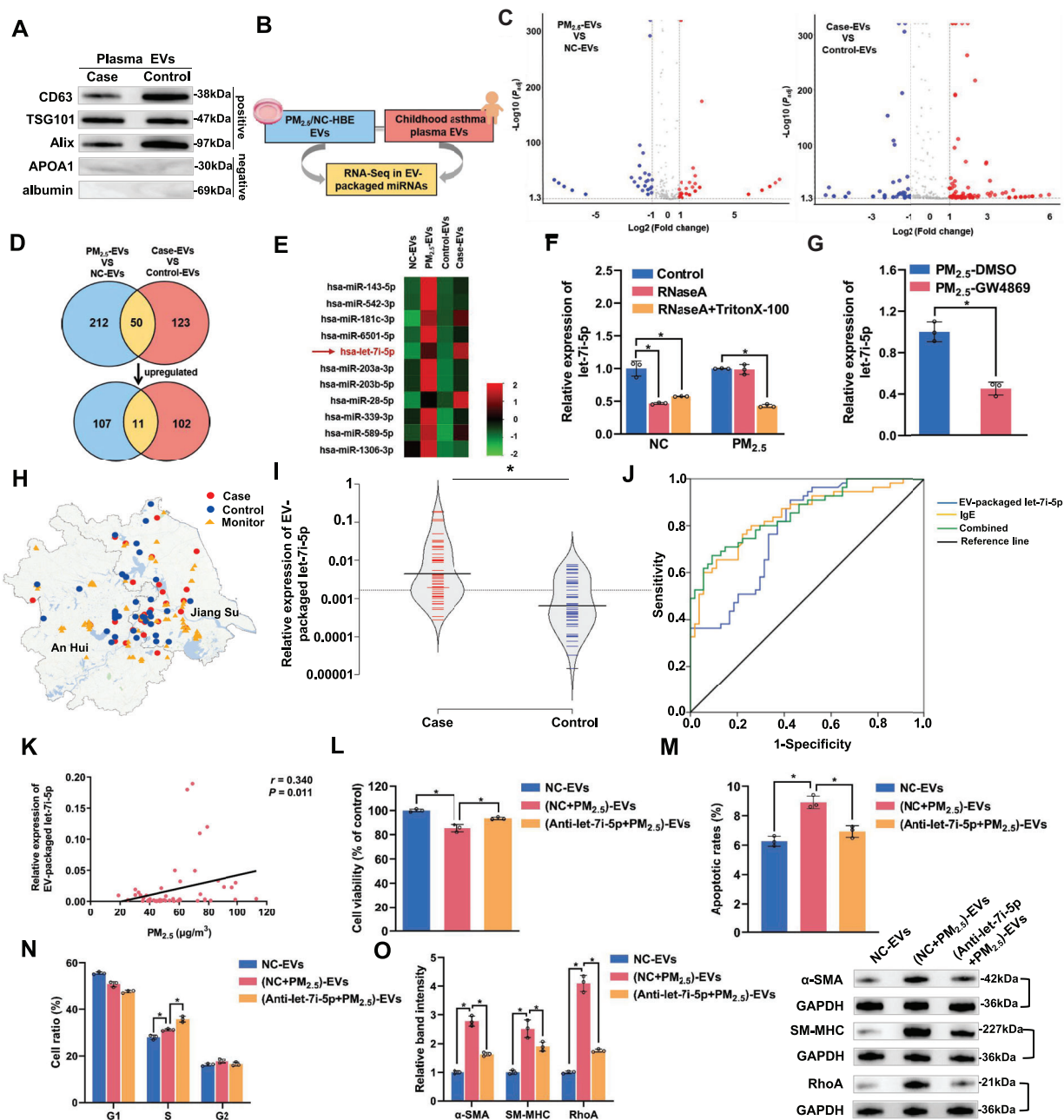


Figure 3. The role of EV-packaged let-7i-5p in children with asthma and the phenotype of recipient cells. HBE cells were transfected with NC- or let-7i-5p inhibitor, exposed to NC/PM_{2.5} and then isolated the corresponding EVs, namely, NC-EVs, (NC+PM_{2.5})-EVs, and (Anti-let-7i-5p+PM_{2.5})-EVs, respectively. A) EV-specific markers (CD63, TSG101 and Alix) and negative controls (APOA1 and albumin) were evaluated using Western blotting. B) Schematic model showing the generation of EV-packaged miRNA expression profiles. C) Volcano plots of different EV-packaged miRNAs in PM_{2.5}-treated HBE cell models and children with asthma. The red and blue plots indicate the differentially expressed EV-packaged miRNAs. D) Venn diagram showing the overlapping upregulated EV-packaged miRNAs. E) Hierarchical clustering analysis of the 11 overlapping upregulated EV-packaged miRNAs identified from the Venn diagram. F) The level of let-7i-5p in the culture medium of PM_{2.5}/NC-treated HBE cells incubated with 2 μg mL⁻¹ RNaseA alone or in combination with 0.1% Triton X-100 was determined using RT-qPCR. G) The level of let-7i-5p in the culture medium of PM_{2.5}-treated HBE cells exposed to DMSO or GW4869 was determined using RT-qPCR. H) Locations of the individuals' residences and air quality monitoring stations. I) The level of plasma EV-packaged let-7i-5p was determined using RT-qPCR. J) ROC curve analysis of plasma levels of EV-packaged let-7i-5p and IgE. K) Correlation analysis was performed between plasma EV-packaged let-7i-5p and PM_{2.5} exposure levels in children with asthma. L) The viability of HBE cells incubated with NC-EVs, (NC+PM_{2.5})-EVs or (Anti-let-7i-5p+PM_{2.5})-EVs was evaluated using a CCK-8 assay. M) The apoptosis of HBE cells incubated with NC-EVs, (NC+PM_{2.5})-EVs or (Anti-let-7i-5p+PM_{2.5})-EVs was assessed using flow cytometry. N) The cell cycle of HBE cells incubated with NC-EVs, (NC+PM_{2.5})-EVs, or (Anti-let-7i-5p+PM_{2.5})-EVs was analyzed using flow cytometry. O) The levels of contractile proteins in sensitive HBSMCs incubated with NC-EVs, (NC+PM_{2.5})-EVs, or (Anti-let-7i-5p+PM_{2.5})-EVs were measured using Western blotting. Statistical significance was assessed using two-tailed Student's *t*-test. Values represent means ± SD. **p* < 0.05.

biological effect of EV-packaged let-7i-5p on recipient HBE cells and sensitive HBSMCs. As shown in Figure 3L–O and Figure S14, Supporting Information, the effect of PM_{2.5}-EVs on enhancing cytotoxicity in HBE cells or increasing the contractility of sensitive HBSMCs was blocked when let-7i-5p within PM_{2.5}-treated HBE cells was antagonized by a let-7i-5p inhibitor. Moreover, the effects of PM_{2.5}-EVs on recipient cells were enhanced when let-7i-5p was overexpressed in recipient cells transfected with the let-7i-5p mimic (Figure S15, Supporting Information). Collectively, these data indicate that EV-packaged let-7i-5p released by PM_{2.5}-treated HBE cells induces cytotoxicity in “horizontal” recipient HBE cells and increases the contractility of “longitudinal” recipient-sensitive HBSMCs.

2.5. Let-7i-5p Is Packaged into EVs via ELAVL1 and Induces Asthma by Activating the MAPK Signaling Pathway

To investigate the mechanism by which let-7i-5p is loaded into EVs, we used the database of RNA-binding protein specificities (RBPDB) to predict the specific interaction between let-7i-5p and the RNA-binding proteins (RBPs) binding motif. As shown in Figure 4A, three RBPs, including ELAV-like protein 1 (ELAVL1), a well-defined RBP for sorting miRNAs into EVs,^[23,24] was predicted to specifically bind let-7i-5p (threshold 0.7). Notably, let-7i-5p FISH and ELAVL1 immunostaining indicated the colocalization of let-7i-5p and ELAVL1 in the cytoplasm of HBE cells (Figure 4B). Consistent with these findings, RNA binding protein immunoprecipitation (RIP) assays confirmed a more obvious interaction between let-7i-5p and ELAVL1 in PM_{2.5}-treated HBE cells than in NC-treated HBE cells (Figure 4C), indicating that let-7i-5p is more likely to interact with ELAVL1 following exposure to PM_{2.5}. Moreover, ELAVL1 was significantly upregulated in PM_{2.5}-treated HBE cells (Figure 4D), and the EV-packaged let-7i-5p level was significantly reduced in cells with ELAVL1 knockdown (Figure 4E and Figure S16, Supporting Information). These findings suggest that ELAVL1 is responsible for the specific loading of let-7i-5p into EVs.

Next, we used three target prediction software programs and performed an overlap analysis to identify 169 putative targets of let-7i-5p (Figure 4F and Figure S17, Supporting Information). The subsequent Kyoto Encyclopedia of Genes and Genomes (KEGG) pathway enrichment analysis revealed consistent biological pathways involved in cellular activities (Figure 4G). Notably, the mitogen-activated protein kinase (MAPK) signaling pathway was previously found to be functionally related to asthma, and among 8 candidate targets, dual-specificity protein phosphatase 1 (DUSP1), a key inhibitor, directly inactivates Jun amino-terminal kinase (JNK), extracellular signal-regulated kinase (ERK), and p38 via dephosphorylation.^[25] Thus, we preferentially selected *DUSP1* as a putative downstream let-7i-5p target gene. As shown in Figure 4H and Figure S18, Supporting Information, let-7i-5p overexpression significantly increased the phosphorylation of JNK, ERK and p38 in recipient cells, similar to treatment with EV-packaged let-7i-5p derived from PM_{2.5}-treated HBE cells. Further dual-luciferase reporter assays showed that let-7i-5p significantly reduced the luciferase activity of the wild-type *DUSP1* 3'-UTR reporter (Figure 4I). Moreover, let-7i-5p overexpression or treatment with EV-packaged let-7i-5p released by PM_{2.5}-treated HBE

cells dramatically inhibited *DUSP1* expression in both normal HBE cells and sensitive HBSMCs (Figure 4J and Figure S19, Supporting Information). Furthermore, *DUSP1* knockdown in recipient cells led to potent activation of the MAPK signaling pathway (Figure 4K and Figure S20, Supporting Information), induced cytotoxicity in HBE cells and increased the contractility of sensitive HBSMCs (Figure S21, Supporting Information). These findings imply that EV-packaged let-7i-5p derived from PM_{2.5}-treated HBE cells may inhibit *DUSP1* expression to increase the phosphorylation of JNK, ERK and p38, thereby activating the MAPK signaling pathway and inducing asthma attacks through both “horizontal” and “longitudinal” mechanisms.

2.6. EV-Packaged Let-7i-5p Mediates PM_{2.5} Exposure-Induced Asthma In Vivo

We established a model of ovalbumin (OVA)-induced asthma in juvenile mice and subjected the mice to the indicated treatments to assess the role of EV-packaged let-7i-5p in PM_{2.5}-induced asthma in vivo (Figure 5A). Consistent with the in vitro observations, treatment with PM_{2.5} or PM_{2.5}+let-7i-5p EVs significantly increased bronchoconstriction (Figure 5B), increased the levels of three contractile proteins (Figure S22, Supporting Information), upregulated EV-packaged let-7i-5p in bronchoalveolar lavage fluid (BALF) (Figure 5C), reduced the *DUSP1* mRNA level in BALF (Figure 5D), and damaged lung tissues (Figure 5E); these effects were accompanied by *DUSP1* downregulation (Figure 5F) and an elevated let-7i-5p level in lung tissues (Figure 5G). Compared with the OVA or OVA+PM_{2.5}+NC-EVs group, the levels of phosphorylated JNK, ERK and p38 were increased in the OVA+PM_{2.5} or OVA+PM_{2.5}+let-7i-5p EVs group (Figure S23, Supporting Information), indicating that EV-packaged let-7i-5p stimulated PM_{2.5}-induced asthma by activating the MAPK signaling pathway. Furthermore, the IL-6 concentration in BALF was significantly increased by the same treatment, further confirming the establishment of the mouse model of OVA-induced asthma (Figure 5H). The observations described the above highlight that EV-packaged let-7i-5p promotes PM_{2.5}-induced airway contraction and cytotoxicity by inhibiting its target gene *DUSP1*.

3. Discussion

In the current study, we first conducted RNA sequencing of EV-packaged miRNAs in plasma from children with asthma and healthy controls and PM_{2.5}/NC-treated HBE cell models, and we identified a novel miRNA, let-7i-5p, expressed at high levels in PM_{2.5}-EVs and plasma from children with asthma. Let-7i-5p was packaged into EVs through an interaction with ELAVL1 and then taken up by “horizontal” recipient normal HBE cells and “longitudinal” recipient-sensitive HBSMCs. Functionally, EV-packaged let-7i-5p activated the MAPK signaling pathway by inhibiting its target gene *DUSP1*, resulting in cytotoxicity in “horizontal” recipient HBE cells and increased contractility of “longitudinal” recipient-sensitive HBSMCs (Figure 5I).

Because the composition of PM_{2.5} is easily affected by the geographical location and meteorological conditions,^[26,27] we used National Institute of Standards and Technology (NIST) reference materials that have a well-characterized chemical content of

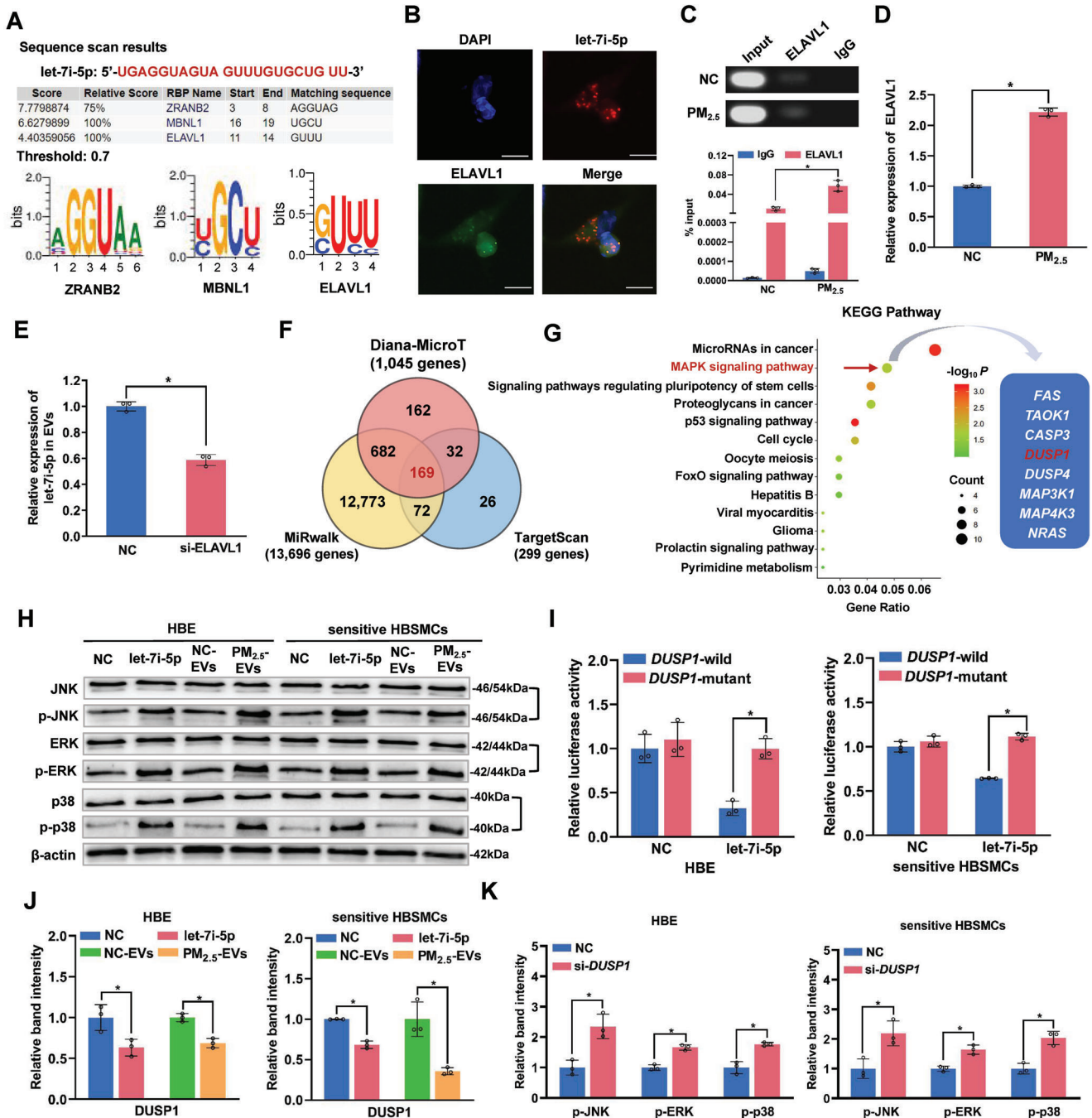


Figure 4. Let-7i-5p is packaged into PM_{2.5}-EVs in an ELAVL1-dependent manner and regulates the *DUSP1* expression level in recipient cells. A) The specific interaction between the let-7i-5p sequence and RNA-binding protein motifs was predicted by RBPDB (threshold value = 0.7). B) Immunofluorescence assessment of let-7i-5p (red) and ELAVL1 (green) colocalization in HBE cells. Scale bar, 20 μm. C) Upper panel: image of gel electrophoresis of PCR products from the RIP assay. Lower panel: an RIP assay with an anti-ELAVL1 antibody or control IgG was performed on PM_{2.5}/NC-treated HBE cells. The level of let-7i-5p in the immunoprecipitates was determined using RT-qPCR. D) The level of the ELAVL1 mRNA in PM_{2.5}/NC-treated HBE cells was determined using RT-qPCR. E) The level of let-7i-5p in EVs derived from HBE cells transfected with si-ELAVL1 was determined using RT-qPCR. F) The potential target genes containing the let-7i-5p seed sequence were predicted using the Diana-MicroT, MiRwalk and TargetScan databases. G) KEGG pathway enrichment analysis of the 169 target genes. H) The protein levels of MAPK pathway-related signaling molecules in NC mimic-, let-7i-5p mimic-, NC-EVs-, or PM_{2.5}-EVs-treated recipient cells (HBE cells and sensitive HBSMCs) were determined using Western blotting. I) The binding affinity of let-7i-5p for *DUSP1* was assessed using a dual-luciferase reporter assay. J) The expression of the *DUSP1* protein in NC mimic-, let-7i-5p mimic-, NC-EVs, or PM_{2.5}-EVs-treated HBE cells (left panel) and sensitive HBSMCs (right panel) was detected using Western blotting. K) The protein levels of MAPK pathway-related signaling molecules in NC- or si-*DUSP1*-transfected HBE cells (left panel) and sensitive HBSMCs (right panel) were determined using Western blotting. Statistical significance was assessed using a two-tailed Student's *t*-test. Values represent means ± SD. **p* < 0.05.

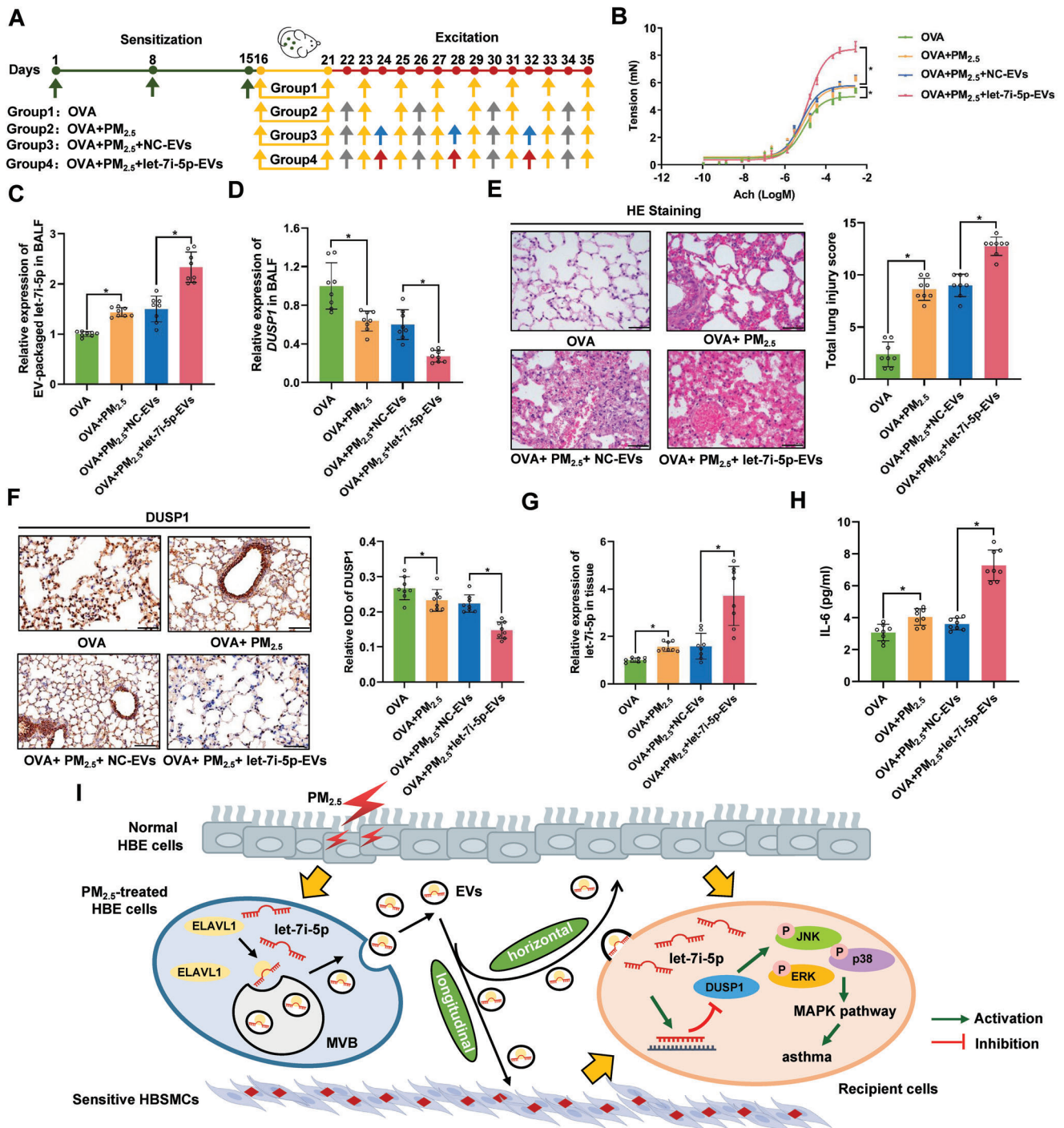


Figure 5. EV-packaged let-7i-5p induces asthma in vivo. Thirty-two female BALB/c mice were randomly assigned to the OVA group (group 1), OVA+PM_{2.5} group (group 2), OVA+PM_{2.5}+NC-EVs group (group 3), or OVA+PM_{2.5}+let-7i-5p-EVs group (group 4). A) Schematic showing the process used to establish the mouse model. The green arrows indicate that each mouse was injected with 28.8 μ L of the OVA suspension containing 3.6 μ g of OVA and 144 μ g of Al(OH)₃. The yellow arrows indicate that mice were exposed to 2% OVA for 20 min. The grey arrows indicate that mice were exposed to 1.57 mg kg⁻¹ PM_{2.5}. The blue arrows indicate that mice were challenged by an endotracheal instillation of 2 μ g of let-7i-5p-EVs. B) Detection of bronchoconstriction using myography. C) The level of EV-packaged let-7i-5p in BALF was determined using RT-qPCR. D) The level of DUSP1 in BALF was determined using RT-qPCR. E) Representative images of H&E staining in lung tissues and total lung injury scores for each group. Scale bar, 50 μ m. F) Representative photographs and quantification of DUSP1 immunostaining in lung tissues. Scale bar, 50 μ m. G) The level of let-7i-5p in lung tissues was determined using RT-qPCR. H) The concentration of IL-6 in BALF was measured using ELISA. I) In the proposed model, EV-packaged let-7i-5p secreted by PM_{2.5}-treated HBE cells induce asthma by regulating the expression of its target gene DUSP1 and activating the MAPK signaling pathway in recipient cells. MVB, multivesicular bodies. Statistical significance was assessed using two-tailed Student's *t*-test. Values represent means \pm SD. * *p* < 0.05.

PM_{2.5} and represent urban PM_{2.5} levels. Our results revealed that PM_{2.5} decreased the viability of normal HBE cells, consistent with our previous studies.^[28] We then hypothesized that PM_{2.5}-treated HBE cells might secrete EVs to regulate the biological function of neighboring or distant cells. Our coculture experiments indicated that EVs released by PM_{2.5}-treated HBE cells may induce cytotoxicity in normal HBE cells. As expected, PM_{2.5}-EVs were efficiently transferred into recipient HBE cells^[29,30] and then “horizontally” induce cytotoxicity in HBE cells; however, this effect was abolished by pretreatment of recipient HBE cells with the EV secretion inhibitor GW4869. The biological effects of PM_{2.5} and PM_{2.5}-EVs on the cell cycle of HBE cells were not consistent because PM_{2.5}-EVs represent the effect of aberrantly expressed intracellular cargos carried by PM_{2.5}-EVs. Similarly, PM_{2.5}-EVs were taken up by recipient-sensitive HBSMCs and subsequently promoted sensitive HBSMC contractility by directly increasing the expression of α -SMA, SM-MHC and RhoA. Thus, PM_{2.5}-EVs play a key role in PM_{2.5}-induced asthma through both “horizontal” and “longitudinal” mechanisms. The air–liquid interface (ALI) model is becoming an efficient and realistic tool for bronchial epithelial toxicity testing following exposure to air pollutants.^[31] A better understanding of the biological function of EV-packaged let-7i-5p in PM_{2.5}-induced asthma based on the ALI model is needed.

Based on RNA sequencing, we determined that let-7i-5p was overexpressed in PM_{2.5}-EVs and plasma-derived EVs from children with asthma and was mainly encapsulated in EVs instead of being freely secreted. Let-7i-5p, a member of the lethal-7 (let-7) miRNA family, has been detected in various tissues and cell types (i.e., lung tissue, smooth muscle, epithelial cells, and macrophages).^[15,32] To date, only one study has reported that let-7i-5p was differentially expressed in bronchial cells from steroid-naive subjects with asthma and was downregulated in patients with asthma,^[25] which is inconsistent with our results. The main explanation for the inconsistency might be the difference in the ages and ethnicity of the subjects. Various studies have indicated that EVs are ideal biomarkers of many diseases; in addition to being stable in body fluids, EVs carry disease-specific functional molecules.^[33] The advantages of EV-packaged let-7i-5p are based on three aspects. First, we determined that plasma EV-packaged let-7i-5p levels were positively correlated with PM_{2.5} exposure in children with asthma, indicating that let-7i-5p is a specific predictor of PM_{2.5}-induced asthma in children. Second, we observed a significant increase in EV-packaged let-7i-5p levels produced by PM_{2.5}-stimulated HBE cells, and EV-packaged let-7i-5p performs crucial functions in effector cells of asthma (HBE and sensitive HBSMCs), which is helpful for both explaining the biological mechanism of PM_{2.5}-induced asthma and further investigating therapeutic approaches. Third, EV-packaged let-7i-5p was stable in plasma and had the ability to discriminate children with asthma from healthy controls with acceptable sensitivity and specificity. These observations imply that EV-packaged let-7i-5p has the potential to serve as a specific biomarker for PM_{2.5}-induced childhood asthma compared with a series of classical predictors. Furthermore, further investigations are needed to determine whether EV-packaged let-7i-5p is related to asthma induced by other allergens.

Interestingly, we revealed that EV-packaged let-7i-5p was delivered into recipient cells and then “horizontally” induced cy-

tototoxicity in HBE cells and “longitudinally” promoted the contractility of sensitive HBSMCs. This conclusion was based on the findings listed below. 1) Let-7i-5p overexpression caused cytotoxicity in HBE cells and increased the expression of contractile proteins in sensitive HBSMCs; 2) HBE cells transfected with Cy3-labelled let-7i-5p mimic were cocultured with recipient cells^[34] to show that EV-packaged let-7i-5p produced by HBE cells was directly transferred into either “horizontal” or “longitudinal” recipient cells; 3) Let-7i-5p overexpression in recipient cells was caused mainly by treatment with PM_{2.5}-EVs rather than by direct exposure to PM_{2.5}; 4) Incubation with (Anti-let-7i-5p+PM_{2.5})-EVs significantly decreased the capacity of PM_{2.5}-EVs to inhibit cytotoxicity in “horizontal” recipient HBE cells and decrease α -SMA, SM-MHC and RhoA expression levels in “longitudinal” recipient-sensitive HBSMCs; and 5) Transfection of the let-7i-5p mimic into recipient cells significantly increased the capacity of PM_{2.5}-EVs to induce asthma. Asthma is driven by a complex cellular communication network composed of multiple cell types.^[10,35] The cell–cell communication of EV-packaged let-7i-5p with other cell types in the cell microenvironment of asthma must be investigated in further studies. Moreover, PM_{2.5} accelerated the production of EV-packaged let-7i-5p by HBE cells by upregulating levels of the EV packaging-related protein ELAVL1 rather than increasing cellular let-7i-5p expression levels. Notably, previous studies have reported that EV-packaged miRNAs are selectively packaged into EVs by several RBPs, including hnRNP2B1, hnRNPQ and ELAVL1.^[23,36,37] Consistent with these results, ELAVL1 (also called HuR) specifically bound let-7i-5p through a specific motif (GUUU) and directed the sorting of let-7i-5p into EVs in the present study, which might suggest unique strategies to eliminate EV-packaged let-7i-5p during PM_{2.5} exposure. In addition to RBPs, Ago2 and Y-box protein 1 have been reported to participate in the EV packaged export of miRNA.^[38,39] Additionally, lncRNA–miRNA interactions have recently been described as a new regulatory mechanism for EV-packaged miRNA export.^[40] Thus, we need to fully elucidate the regulatory mechanism in further studies.

The MAPK signaling pathway is involved in almost all aspects of asthma pathophysiology, and its activity is self-adjusting between phosphorylation and dephosphorylation.^[41,42] Extracellular stimulation (by environmental exposure, growth factors or proinflammatory cytokines) leads mainly to the activation of the three main MAPK signaling pathway modules: JNK, ERK and p38.^[43] Here, we found that EV-packaged let-7i-5p secreted by PM_{2.5}-treated HBE cells increased the levels of phosphorylated JNK, ERK and p38 by suppressing the expression of the let-7i-5p target gene *DUSP1* in both HBE cells and sensitive HBSMCs, thereby activating the MAPK signaling pathway to induce asthma. Consistent with our in vitro results, juvenile mice treated with EV-packaged let-7i-5p exhibited more severe bronchial contraction, higher levels of EV-packaged let-7i-5p in BALF and lower *DUSP1* protein levels in lung tissues compared to those in control mice (OVA group or OVA+PM_{2.5}+NC-EVs group). Because all the functions we investigated were based on OVA-induced asthmatic mouse models treated with PM_{2.5}, OVA and PM_{2.5} could be used as internal controls for the OVA+PM_{2.5}+NC/let-7i-5p EVs group, thereby eliminating the effect of OVA or PM_{2.5} on target molecules and other indices. Interestingly, EV-packaged let-7i-5p regulated the MAPK signaling pathway through the

target gene *DUSP1* and increased IL-6 expression levels. These results indicate that EV-packaged let-7i-5p may regulate the release of inflammatory factors. Thus, studies exploring the function of let-7i-5p in inflammatory cells are urgently needed. Due to the lower amount of plasma in the juvenile mouse model, we were unable to detect plasma EV-packaged let-7i-5p in vivo. We therefore isolated BALF samples in vivo to measure the expression of EV-packaged let-7i-5p. Overexpression and knockout of let-7i-5p in mice exposed to OVA and PM_{2.5} are necessary controls to further verify the biological effects of EV-packaged let-7i-5p on PM_{2.5}-induced asthma. Moreover, the CRISPR/Cas9 system will be used to generate let-7i-5p knockout cell lines, thereby further validating the effect of EV-packaged let-7i-5p on PM_{2.5}-induced asthma in vivo and in vitro. House dust mites (HDMs), important natural allergens, have been shown to more closely mimic human asthma than OVA when constructing an asthmatic mouse model.^[44] Therefore, we will use the HDM-induced asthmatic mouse model to further validate our results.

In summary, our findings provide evidence of a mechanism underlying PM_{2.5}-induced childhood asthma in which EV-packaged let-7i-5p “horizontally” induces cytotoxicity in HBE cells and “longitudinally” promotes the contractility of sensitive HBSMCs by inhibiting the expression of its target gene *DUSP1*. In addition, EV-packaged let-7i-5p was upregulated in the plasma of children with asthma, and the EV-packaged let-7i-5p level was positively correlated with PM_{2.5} exposure. Our results not only revealed a crucial mechanism of EV-packaged miRNA-regulated cell–cell communication from PM_{2.5}-treated HBE cells to recipient cells to induce asthma, but also opened a new avenue for a diagnostic strategy and therapeutic approach for asthma in children exposed to high levels of PM_{2.5}.

4. Experimental Section

Study Subjects and Clinical Samples: Beginning in July 2017, the authors recruited 110 children from Children’s Hospital of Nanjing Medical University (Nanjing, China) and collected their plasma samples. Children with asthma were diagnosed according to the guidelines for the diagnosis, prevention and treatment of childhood asthma (2016 edition) formulated by the Chinese Medical Association. During the same period, non-asthmatic children who were age- and sex-matched by the frequency with the cases were selected as healthy controls. Written informed consent forms were signed by the children and their parents, and the study protocol was approved by the Ethics Committee of Nanjing Medical University (2017-392).

PM_{2.5} Exposure Assessment: The PM_{2.5} concentration distribution was obtained from China National Environmental Monitoring Center (CNEMC) data provided by Qingyue Data (<https://data.epmap.org>). The PM_{2.5} concentration at the site 30 days before recruitment of the subjects into this study was recorded as the average concentration in the case-control study. XGeocoding software was utilized to obtain the latitude and longitude of the subjects’ residence and monitoring sites. Inverse distance weighted interpolation (IDW) is an important spatial interpolation method in ArcGIS software (version 10.2), that was employed to evaluate the individual PM_{2.5} exposure concentrations.^[45,46] The details are explained as follows:

$$Z(u) = \frac{\sum_{i=1}^n \frac{1}{d^p} z(u_i)}{\sum_{i=1}^n \frac{1}{d^p}} \quad (1)$$

in Equation (1), $Z(u)$ denotes the PM_{2.5} exposure concentration of subjects, $z(u_i)$ is the observed value at the n measured sites, and d^p

represents the inverse distance weighted interpolation (IDW) weight distance.

Treatment of Recipient Cells with PM_{2.5}: Standard reference material 2786 (SRM2786) from the NIST was used as the PM_{2.5} reference in this study.^[28] The PM_{2.5} standard was suspended in culture medium at a concentration of 2 mg mL⁻¹. When recipient cells reached 50–60% confluence at the bottom of the petri dish, recipient cells were treated with different concentrations (0, 31.25, 62.5, 125, 250, 500, 1000, or 1500 μg mL⁻¹) of the stock PM_{2.5} standard suspension for 12, 24 or 48 h.^[47]

EV Isolation, Characterization, and Internalization: EVs were isolated from the culture medium of HBE cells with an ExoQuick TC Kit (SBI, USA), and EVs were purified from the plasma of children using an ExoQuick Plasma Prep with Thrombin Kit (SBI, USA). The shape and size of EVs were assessed using transmission electron microscopy (TEM) (Technai G2, FEI, USA). The size distribution of EVs was quantified using nanoflow cytometry (NanoFCM) with a U30 Flow NanoAnalyzer (NanoFCM, Inc., China) and technical assistance provided by KeyGEN Biotech Co. Ltd (Jiangsu Province, China). Western blotting was utilized to detect the EV protein markers CD63 (antibody: ab134045, Abcam, USA), TSG101 (antibody: ab125011, Abcam, USA) and Alix (antibody: 92880, CST, USA), and the negative controls calnexin (antibody: ab133615, Abcam, USA), Grp94 (antibody: ab108606, Abcam, USA), APOA1 (antibody: ab52945, Abcam, USA), and albumin (antibody: ab207327, Abcam, USA) to confirm that active substances isolated from culture medium or plasma were EVs. The 2 μg of PM_{2.5}/NC-EVs diluted with 200 μL of PBS were extracted (100 μL) and then labelled with 4 μL of PKH67 (green fluorescence; Sigma, USA) and 1 mL Diluent C (Sigma, USA). After an incubation for 4 min at room temperature, PM_{2.5}/NC-EV labelling was terminated by the addition of 2 mL of 0.5% bovine serum albumin (BSA). Dyed EVs were isolated from the above staining liquid using an ExoQuick TC Kit to remove unbound dye from the PKH67-labelled PM_{2.5}/NC-EVs. The dyed EVs were added to recipient cells and incubated for 3 h. Fluorescence microscopy (Zeiss, Germany) was used to visualize PKH67-labelled EVs in recipient cells. The details of this protocol are described in the authors’ previous study.^[30]

EV Treatment: The concentration of EVs was determined with a bicinchoninic acid (BCA) protein assay kit (Beyotime Institute of Biotechnology, China). For in vitro treatment, 2 μg of EVs (equivalent to $\approx 1 \times 10^7$ of the indicated HBE cells) were incubated with 2×10^5 recipient cells for 24 h. EV secretion was inhibited by pretreating normal HBE cells with 20 μM GW4869 (Sigma, USA) or 0.005% DMSO (Sigma, USA) as a control for 6 h and then exposing cells to the PM_{2.5} standard for 24 h. The culture medium of these cells was prepared for EV isolation or RNA extraction. The indicated HBE cells were treated with 2 μg mL⁻¹ RNaseA (Beyotime Institute of Biotechnology, China) alone or in combination with 0.1% Triton X-100 (Beyotime Institute of Biotechnology, China) for 30 min, and the expression of miRNAs in the culture medium of HBE cells was detected using real-time fluorescence quantitative polymerase chain reaction (RT-qPCR) to investigate the expression pattern of extracellular miRNAs.

Analysis of the EV-Packaged miRNA Expression Profile: EV-packaged RNA was isolated from the plasma of children with asthma or non-asthmatic children, from which two pooled plasma samples of 4.8 mL each (4.8 mL = 8 samples \times 600 μL/sample) were obtained (Table S3, Supporting Information). Moreover, EV-packaged RNA was isolated from the culture medium of PM_{2.5}/NC-treated HBE cells. The EV-packaged miRNA expression profiles of plasma from children and culture medium from the cell models were generated with the Illumina HiSeq 2500 platform (Novogene Co., Ltd., China).

Western Blot Analysis: The indicated cells or EV-packaged lysates were obtained using RIPA lysis buffer mixed with 0.5% PMSF and centrifuged at 15,000 rpm for 15 min at 4 °C. Protein concentrations were determined using the BCA kit. Equal amounts of protein (60 μg) were separated by sodium dodecyl sulfate–polyacrylamide gel electrophoresis (SDS-PAGE) and transferred to polyvinylidene fluoride (PVDF) membranes. Subsequently, membranes were incubated overnight at 4 °C with anti- α -SMA (19245, CST, USA), anti-SM-MHC (ab53219, Abcam, USA), anti-RhoA (2117, CST, USA), anti-ELAVL1 (ab200342, Abcam, USA), anti-DUSP1 (2455724, Millipore, USA), anti-MAPK family (9926, CST, USA), or anti-phospho-MAPK family (9910, CST, USA) antibodies. Glyceraldehyde

phosphate dehydrogenase (GAPDH) and β -actin were used as loading controls for normalization. Immunoreactive proteins were examined using a Bio-Rad gel imaging system (Bio-Rad, USA).

Establishment of the Juvenile Mouse Model of Asthma: Thirty-two juvenile BALB/c mice (3 weeks old, female) were randomly divided into four groups of eight mice per group: the OVA group (OVA), OVA+PM_{2.5} exposure group (OVA+PM_{2.5}), OVA+PM_{2.5} exposure+NC-EVs injection group (OVA+PM_{2.5}+NC-EVs), and OVA+PM_{2.5} exposure+let-7i-5p-EVs injection group (OVA+PM_{2.5}+let-7i-5p-EVs). On days 1, 8 and 15, juvenile mice in the four groups were intraperitoneally injected with 0.2 mL of the OVA suspension containing 25 μ g of OVA (Sigma, USA) and 1 mg of Al(OH)₃ (Aladdin, China). All mice were then exposed to nebulized 2% OVA on days 16–21, 23, 25, 27, 29, 31, 33, and 35 (20 min each time). Juvenile mice in all groups except the OVA group were exposed to 1.57 mg kg⁻¹ nebulized PM_{2.5} on days 22, 26, 30, and 34. Additionally, mice in the OVA+PM_{2.5}+NC/let-7i-5p-EVs group received NC/let-7i-5p EVs (2 μ g/sample) via intraperitoneal injection on days 24, 28 and 32. All animal studies were approved by the Institutional Animal Care and Use Committee of Nanjing Medical University (IACUC-2004036).

Statistical Analysis: Significant differences between the two groups were analyzed using Student's *t*-test or Pearson's χ^2 test. The ROC curve was analyzed to obtain the AUC values and evaluate the capability for discriminating cases from healthy controls. Spearman's correlation analysis was utilized to determine the relationship between PM_{2.5} exposure and the plasma level of EV-packaged let-7i-5p. Three target prediction software programs, Diana-MicroT, MiRwalk and TargetScan, were used to predict putative targets of let-7i-5p. KEGG pathway analyses were performed with Database for Annotation, Visualization and Integrated Discovery (DAVID) 6.8 software (<https://david-d.ncifcrf.gov/>) to identify the main biological pathways of the differentially expressed genes. RBPDB (<http://rbpdb.ccb.utoronto.ca/>) was used to predict the interaction between motifs of RBPs and let-7i-5p.^[48] $p < 0.05$ was considered statistically significant. All experiments were replicated at least three times. Quantitative data are presented as the means \pm standard deviations (SD). Statistical analyses were performed with SAS 9.1.3 software (SAS Institute, Inc., USA). Additional experimental methods are described in the Supporting Information Materials and Methods.

Supporting Information

Supporting Information is available from the Wiley Online Library or from the author.

Acknowledgements

This study was supported in part by National Natural Science Foundation of China (81973095, 82130096), Natural Science Foundation of Jiangsu Province (BE2019729, BK20181120), China Postdoctoral Science Foundation funded project (2020M681673), and the Priority Academic Program Development of Jiangsu Higher Education Institutions (Public Health and Preventive Medicine). The authors are grateful to all the people who helped them accomplish this project. They thank Qingyue Data (<https://data.epmap.org>) for support on Environmental data processing.

Author's Contributions

R.Z., M.D., and M.T. contributed equally to this work. Z.Z., M.W., and M.D. designed and supervised the study. M.T., R.Z., C.G., R.X., and H.C. contributed to collect the characteristics of subjects and recruit study subjects. R.Z., C.W., J.L., F.G., and Z.M. contributed to the functional experiments. R.Z., M.D., and Z.Z. prepared the manuscript.

Conflict of Interest

The authors declare no conflict of interest.

Data Availability Statement

The data that support the findings of this study are available from the corresponding author upon reasonable request.

Keywords

PM_{2.5}, childhood asthma, extracellular vesicles, let-7i-5p, MAPK signaling pathway

Received: June 10, 2021

Revised: October 9, 2021

Published online: November 23, 2021

- [1] P. W. Hekking, R. R. Wener, M. Amelink, A. H. Zwinderman, M. L. Bouvy, E. H. Bel, *J. Allergy Clin. Immunol.* **2015**, *135*, 896.
- [2] H. W. Hallas, B. L. Chawes, M. A. Rasmussen, L. Arianto, J. Stokholm, K. Bønnelykke, H. Bisgaard, *PLoS Med.* **2019**, *16*, e1002722.
- [3] *Lancet Respir. Med.* **2017**, *5*, 691.
- [4] *Lancet* **2018**, *392*, 1736.
- [5] A. Papi, C. Brightling, S. E. Pedersen, H. K. Reddel, *Lancet* **2018**, *391*, 783.
- [6] F. Chen, Z. Lin, R. Chen, D. Norback, C. Liu, H. Kan, Q. Deng, C. Huang, Y. Hu, Z. Zou, W. Liu, J. Wang, C. Lu, H. Qian, X. Yang, X. Zhang, F. Qu, J. Sundell, Y. Zhang, B. Li, Y. Sun, Z. Zhao, *Environ. Pollut.* **2018**, *232*, 329.
- [7] E. Garcia, K. T. Berhane, T. Islam, R. McConnell, R. Urman, Z. Chen, F. D. Gilliland, *JAMA, J. Am. Med. Assoc.* **2019**, *321*, 1906.
- [8] W. Gao, L. Li, Y. Wang, S. Zhang, I. M. Adcock, P. J. Barnes, M. Huang, X. Yao, *Respirology* **2015**, *20*, 722.
- [9] I. Bara, A. Ozier, J.-M. T. De Lara, R. Marthan, P. Berger, *Eur. Respir. J.* **2010**, *36*, 1174.
- [10] D. J. Erle, D. Sheppard, *J. Cell Biol.* **2014**, *205*, 621.
- [11] A. A. Farooqi, N. N. Desai, M. Z. Qureshi, D. R. N. Librelotto, M. L. Gasparri, A. Bishayee, S. M. Nabavi, V. Curti, M. Daglia, *Biotechnol. Adv.* **2018**, *36*, 328.
- [12] R. Xu, D. W. Greening, H.-J. Zhu, N. Takahashi, R. J. Simpson, *J. Clin. Invest.* **2016**, *126*, 1152.
- [13] D. M. Pegtel, S. J. Gould, *Annu. Rev. Biochem.* **2019**, *88*, 487.
- [14] R. Kalluri, V. S. Lebleu, *Science* **2020**, *367*, eaau6977.
- [15] B. Sastre, J. A. Cañas, J. M. Rodrigo-Muñoz, V. Del Pozo, *Front. Immunol.* **2017**, *8*, 826.
- [16] J. Li, Q. Zhou, Y. Liang, W. Pan, Y. Bei, Y. Zhang, J. Wang, Z. Jiao, *Ann. Transl. Med.* **2018**, *6*, 209.
- [17] L. Song, D. Li, X. Li, L. Ma, X. Bai, Z. Wen, X. Zhang, D. Chen, L. Peng, *Environ. Toxicol. Pharmacol.* **2017**, *50*, 192.
- [18] Y. Hu, G. Jin, B. Li, Y. Chen, L. Zhong, G. Chen, X. Chen, J. Zhong, W. Liao, Y. Liao, Y. Wang, J. Bin, *Clin. Sci.* **2019**, *133*, 425.
- [19] J. Jin, F. Qian, D. Zheng, W. He, J. Gong, Q. He, *Int. J. Nanomed.* **2021**, *16*, 3565.
- [20] Z. Shi, S. K. Y. To, S. Zhang, S. Deng, M. Artemenko, M. Zhang, J. Tang, J.-Z. Zeng, A. S. T. Wong, *Theranostics* **2021**, *11*, 3376.
- [21] H. D. Yang, H. S. Kim, S. Y. Kim, M. J. Na, G. Yang, J. W. Eun, H. J. Wang, J. Y. Cheong, W. S. Park, S. W. Nam, *Hepatology* **2019**, *70*, 1262.
- [22] X. Ding, M. Wang, H. Chu, M. Chu, T. Na, Y. Wen, D. Wu, B. Han, Z. Bai, W. Chen, J. Yuan, T. Wu, Z. Hu, Z. Zhang, H. Shen, *Toxicol. Lett.* **2014**, *228*, 25.
- [23] Z. Li, X. Zhou, M. Wei, X. Gao, L. Zhao, R. Shi, W. Sun, Y. Duan, G. Yang, L. Yuan, *Nano Lett.* **2019**, *19*, 19.
- [24] Y. Shi, Z. Wang, X. Zhu, L. Chen, Y. Ma, J. Wang, X. Yang, Z. Liu, *Int. J. Clin. Oncol.* **2020**, *25*, 89.

- [25] O. D. Solberg, E. J. Ostrin, M. I. Love, J. C. Peng, N. R. Bhakta, L. Hou, C. Nguyen, M. Solon, C. Nguyen, A. J. Barczak, L. T. Zlock, D. P. Blagev, W. E. Finkbeiner, K. M. Ansel, J. R. Arron, D. J. Erle, P. G. Woodruff, *Am J. Respir. Crit. Care Med.* **2012**, *186*, 965.
- [26] K. Sawyer, S. Mundandhara, A. J. Ghio, M. C. Madden, *J. Toxicol. Environ. Health, Part A* **2010**, *73*, 41.
- [27] S. Becker, L. A. Dailey, J. M. Soukup, S. C. Grambow, R. B. Devlin, Y.-C. T. Huang, *Environ. Health Perspect.* **2005**, *113*, 1032.
- [28] Q. Yuan, H. Zhu, H. Liu, M. Wang, H. Chu, Z. Zhang, *J. Hazard. Mater.* **2021**, *415*, 125573.
- [29] Y. Liu, F. Luo, B. Wang, H. Li, Y. Xu, X. Liu, L. Shi, X. Lu, W. Xu, L. Lu, Y. Qin, Q. Xiang, Q. Liu, *Cancer Lett.* **2016**, *370*, 125.
- [30] R. Zheng, M. Du, X. Wang, W. Xu, J. Liang, W. Wang, Q. Lv, C. Qin, H. Chu, M. Wang, L. Yuan, J. Qian, Z. Zhang, *Mol. Cancer* **2018**, *17*, 143.
- [31] S. Upadhyay, L. Palmberg, *Toxicol. Sci.* **2018**, *164*, 21.
- [32] H. Lee, S. Han, C. S. Kwon, D. Lee, *Protein Cell* **2016**, *7*, 100.
- [33] S. Stremersch, S. C. De Smedt, K. Raemdonck, *J. Controlled Release* **2016**, *244*, 167.
- [34] W. Ying, M. Riopel, G. Bandyopadhyay, Y. Dong, A. Birmingham, J. B. Seo, J. M. Ofrecio, J. Wollam, A. Hernandez-Carretero, W. Fu, P. Li, J. M. Olefsky, *Cell* **2017**, *171*, 372.
- [35] J. T. Olin, M. E. Wechsler, *BMJ* **2014**, *349*, g5517.
- [36] C. Villarroya-Beltri, C. Gutiérrez-Vázquez, F. Sánchez-Cabo, D. Pérez-Hernández, J. Vázquez, N. Martín-Cofreces, D. J. Martínez-Herrera, A. Pascual-Montano, M. Mittelbrunn, F. Sánchez-Madrid, *Nat. Commun.* **2013**, *4*, 2980.
- [37] L. Santangelo, G. Giurato, C. Cicchini, C. Montaldo, C. Mancone, R. Tarallo, C. Battistelli, T. Alonzi, A. Weisz, M. Tripodi, *Cell Rep.* **2016**, *17*, 799.
- [38] J. Guduric-Fuchs, A. O'connor, B. Camp, C. L. O'neill, R. J. Medina, D. A. Simpson, *BMC Genomics* **2012**, *13*, 357.
- [39] M. J. Shurtleff, M. M. Temoche-Diaz, K. V. Karflis, S. Ri, R. Schekman, *eLife* **2016**, *5*, e19276.
- [40] L. Qu, J. Ding, C. Chen, Z.-J. Wu, B. Liu, Y. Gao, W. Chen, F. Liu, W. Sun, X.-F. Li, X. Wang, Y. Wang, Z.-Y. Xu, L. Gao, Q. Yang, B. Xu, Y.-M. Li, Z.-Y. Fang, Z.-P. Xu, Y. Bao, D.-S. Wu, X. Miao, H.-Y. Sun, Y.-H. Sun, H.-Y. Wang, L.-H. Wang, *Cancer Cell* **2016**, *29*, 653.
- [41] M. Khorasanizadeh, M. Eskian, E. W. Gelfand, N. Rezaei, *Pharmacol. Ther.* **2017**, *174*, 112.
- [42] R. Newton, M. A. Giembycz, *Br. J. Pharmacol.* **2016**, *173*, 3405.
- [43] G. Pelaia, G. Cuda, A. Vatrella, L. Gallelli, M. Caraglia, M. Marra, A. Abbruzzese, M. Caputi, R. Maselli, F. S. Costanzo, S. A. Marsico, *J. Cell. Physiol.* **2005**, *202*, 642.
- [44] B. N. Lambrecht, H. Hammad, J. V. Fahy, *Immunity* **2019**, *50*, 975.
- [45] T. M. Miliillo, J. A. Gardella, *Anal. Chem.* **2008**, *80*, 4896.
- [46] Y. Ramos, B. St-Onge, J.-P. Blanchet, A. Smargiassi, *J. Exposure Sci. Environ. Epidemiol.* **2016**, *26*, 405.
- [47] Q. Xiong, Q. Ru, L. Chen, K. Yue, X. Tian, B. Ma, L. Liu, R. Wu, C. Xu, M. Pi, C. Li, *J. Toxicol. Environ. Health, Part A* **2015**, *78*, 443.
- [48] K. B. Cook, H. Kazan, K. Zuberi, Q. Morris, T. R. Hughes, *Nucleic Acids Res.* **2011**, *39*, D301.